Improvement in Transformer Differential Protection using Singular Value Decomposition

Het Bhalja[1], Bhavesh R. Bhalja[2] and Pramod Agarwal[3]
Department of Electrical Engineering
Indian Institute of Technology Roorkee
Roorkee, India
het_b@ee.iitr.ac.in[1], bhavesh.bhalja@ee.iitr.ac.in[2], pramod.agarwal@ee.iitr.ac.in[3]

***Abstract*— This paper presents a new transformer differential protection technique based on singular value decomposition (SVD). Initially, transformer winding currents are converted into their respective real-time series hankel matrix, and the SVD of that matrix is calculated. The singular values of the transformer winding current on the primary and secondary sides are compared and used to detect internal faults in the transformer. The suggested SVD-based method is not only capable of detecting fault conditions faster than conventional differential protection scheme but also able to restrain its operation during magnetizing inrush, overexcitation, and CT saturation during a heavy through fault. The performance of the proposed scheme is evaluated using numerous simulation cases as well as practical field data. The simulation cases are generated by modelling the existing power system network in PSCAD/EMTDC software, and the protection scheme is developed in a MATLAB environment. The proposed scheme's average response time to detect internal fault is 5 ms, which is faster than the conventional differential protection scheme, indicating the superiority of the proposed method.**

Keywords—Hankel Matrix, Singular Value Decomposition, Transformer Differential Protection

I. Introduction

Transformers are essential equipment in an electrical network because they allow for the bidirectional flow of power with changes in voltage level while maintaining a constant frequency [1]. An internal fault in a transformer can cause catastrophic damage to the equipment and jeopardise the electrical network's stability. The internal faults of the transformer must be detected immediately. As a result, a fast-acting protection scheme is required to respond faster after the inception of the fault. Furthermore, the operation of this protection scheme should be restricted in the event of abnormal operating conditions of the transformer such as magnetic inrush, overexcitation and external fault with CT saturation [2].

The conventional transformer differential protection scheme is still widely used today to protect transformers from internal faults [2]. The operation of a differential protection scheme is governed by the differential protection's two-slope characteristics. The harmonic restrain/blocking methods are widely used to prevent mal-operation during abnormal operating conditions [3]. It uses the second and fifth harmonic of the transformer differential currents to limit its operation during magnetising inrush current and overexcitation conditions [1]-[4]. For restraint, the selective harmonic blocking technique outperforms the harmonic restrain method [3]. However, introducing better magnetic materials in the core reduces harmonic content during inrush, making it harder to determine a suitable threshold [4]. This protection scheme's operating time is approximately one cycle (20 ms) [1]-[2], which is slower than some newly developed protection techniques. Furthermore, these techniques should provide the same level of stability as the traditional differential protection scheme. As a result, there is a need to develop/modify a current protection technique that can provide a faster response time while also having the same level of stability.

The wavelet transform [5]-[6], S-transform [7], Statistical Methods [8]-[10], search-coil based method [11], artificial intelligence (AI) [12]-[13] and neural network (NN) [14], Fuzzy logic [15], Modified differential protection [16]-[19], and other techniques were used by the researchers. Some protection techniques require voltage as an input quantity, which increases the cost of the protection equipment (in the form of an additional voltage/potential transformer) [20]. The search coil-based methods [11] are constrained by the location and placement of the search coils within the transformer winding, as well as the number of search coils used in the protection. The wavelet-based method [5]-[6] has the versatile issue of requiring a higher sampling frequency and being susceptible to external measurement noises. AI [12]-[13] and NN [14] methods need a more significant number of data sets to train the algorithms, and the physical hardware implementation is complex. Methods based on the S-transform [7], [8]-[10] are complex and necessitate a higher level of computational complexity. Because of this limitation, there is still a need to investigate a transformer protection scheme. Some other methods are depicted in [21]-[23] which utilizes novel approaches to the transformer protection problem.

In this paper, the proposed method utilises singular value decomposition (SVD) of the respective hankel matrix of the respective currents of the transformer. The hankel matrix represents time series data (transformer winding currents in this case) into matrix form and then SVD of the individual currents are calculated. After calculating the singular values of the current, it was sorted in descending order and the first-order derivative of the original signal was selected and the difference of singular values (DSV) of the first-order derivative of the respective phase currents on primary and secondary are calculated and the same is used to differentiate between normal operating conditions from abnormal/faulty condition. Furthermore, to detect magnetizing inrush, overexcitation and CT saturation condition during external through fault, separate criteria is developed based on the variance of the normalised differential current (VID) of the respective phase winding of the transformer. The proposed scheme is validated on the power system network simulated in PSCAD/EMTDC and real field data. Numerous cases suggest that the response time of the proposed method is faster (5 ms) than the conventional method for the same case. A comparative analysis of the proposed method with the conventional differential protection scheme is also shown. The concept of SVD along with the hankel matrix and the philosophy of the proposed method is discussed in sections II and III, respectively. The performance evaluation of the proposed method is discussed in section IV.

978-1-7281-7025-1/23/$31.00 ©2023 IEEE
DOI 10.1109/GTD49768.2023.00068

II. METHODOLOGY

A. Hankel Matrix

If we take a one-dimensional time measurement, we get sampled current data for a specific time window. This hankel matrix is built by staking up time-shifted copies of the measurement as rows of this hankel matrix. Because each raw of the hankel matrix represents a time-shifted version of the measurement, forming its hankel matrix yields a set of time-delayed coordinates. In other words, the hankel matrix has identical elements along the anti-diagonals. The $(i,j)^{th}$ element of the hankel matrix will be function of $i+j$. where, i and j are the row and column of the matrix. This hankel matrix can be used to determine the singularity of the measurement signal [23].

Each transformer phase winding current is a one-dimensional time-series signal that can be represented by eq. (1), where N denotes the total number of samples in a given data window.

$$I_{\text{winding}} = [i_1, i_2, i_3, ..., i_p, ..., i_q, ..., i_N] \quad (1)$$

The hankel matrix for the one-dimensional signal is shown in eq. (1) and it can be generated by arranging time series data in a time-delayed fashion in each row of the matrix [23]. The newly developed hankel matrix can be visualised in terms of eq. (2). Where I_{H} is the hankel matrix generated for (1).

$$I_{\text{H}} = \begin{bmatrix} i_1 & i_2 & i_3 & \dots & i_p \\ i_2 & i_3 & \dots & i_p & i_{p+1} \\ \vdots & \vdots & \vdots & \vdots & \vdots \\ i_q & i_{q+1} & \dots & \dots & i_{\text{N}} \end{bmatrix} \quad (2)$$

B. Singular Value Decomposition

The singular value decomposition (SVD) is a data-driven Fourier transform generalisation that can be tailored to the specific problem or data. The SVD is a widely used tool in linear algebra for data processing that also serves as the foundation for many machine learning algorithms. So, the SVD is a data reduction tool that can reduce data into key features required for analysing, understanding, and describing the data. It can find key features or relations between the data being analysed.

Now to calculate the SVD of the hankel matrix (H), it can be visualised as per (3),

$$\text{H} = \text{U} \times \sum \times \text{V}^{\text{T}} \quad (3)$$

Where, U and V are orthogonal matrices and $\sum$ is diagonal matrices. The U and V can be represented as column vectors, with U = [u_1, u_2, …, u_m] and V = [v_1, v_2, …, v_n]. The diagonal elements of the matrix are {s_1, s_2, …, s_n}. Furthermore, the diagonal elements are the singular values of the matrix H and they follow the relationship $s_1 \geq s_2 \geq \ldots \geq s_n$. The linear combination of the signals can thus represent the original signal as per (4). This approach does not require whole cycle data for fault identification and fault feature extraction, resulting in a faster response to the Fourier transform technique.

$$\text{H} = \text{U} \times \sum \times \text{V}^{\text{T}} = \sum_{i=1}^{n} s_n u_n v_n^{\text{T}} = s_1 u_1 v_1^{\text{T}} + s_2 u_2 v_2^{\text{T}} + \ldots + s_{\text{n}} u_n v_n^{\text{T}} \quad (4)$$

The singular values of the matrix H can be calculated by following the steps. Before starting the process, we have the relation that $\text{H} = \text{U} \times \sum \times \text{V}^{\text{T}}$ and the steps to calculate the singular values are mentioned below,

$$\text{H}^{\text{T}}\text{H} = (\text{U} \sum \text{V}^{\text{T}})^{\text{T}} \ \text{U} \sum \text{V}^{\text{T}} \quad (5)$$

$$\text{H}^{\text{T}}\text{H} = \text{V} \sum^{\text{T}} \text{U}^{\text{T}} \times \text{U} \sum \text{V}^{\text{T}} = \text{V} \sum^{\text{T}} (\text{U}^{\text{T}}\text{U}) \sum \text{V}^{\text{T}} \quad (6)$$

$$\text{H}^{\text{T}}\text{H} = \text{V} \sum^{\text{T}} (\text{I}) \sum \text{V}^{\text{T}} = \text{V}(\sum^{\text{T}} \sum) \text{V}^{\text{T}} \quad \because \text{U}^{\text{T}}\text{U} = \text{I} \quad (7)$$

Now, $\text{U}^{\text{T}}\text{U}$ will be an identity matrix (I) because U and V are orthogonal matrices. Further, eq. (7) can be written as,

$$\text{V}(\sum^{\text{T}} \sum) \text{V}^{\text{T}} = \text{V}(\lambda) \text{V}^{\text{T}} \ \Rightarrow \ \sum^{\text{T}} \sum = \lambda \quad (8)$$

Where λ is the eigenvalues and V is the eigenvectors of the $\text{H}^{\text{T}}\text{H}$. So it can be interpreted from eq. (8) that,

$$\sum^{\text{T}} \sum = [\text{diag}\{s_1^2, s_2^2, ..., s_n^2\}] \ \& \ \lambda = [\text{diag}\{\lambda_1, \lambda_2, ..., \lambda_n\}] \quad (9)$$

$$\therefore \{s_1, s_2, ..., s_n\} = \{\sqrt{\lambda_1}, \sqrt{\lambda_2}, ..., \sqrt{\lambda_n}\} \quad (10)$$

Similarly, HH^{T} can likewise produce the same values. The positive eigenvalues of the $\text{H}^{\text{T}}\text{H}$ or HH^{T} are directly related to the singular values of H according to the foregoing derivation (eq. (5) to (10)). The k^{th} singular value of the signal can be used to find the $(k\text{-}1)^{th}$ order derivative of the original signal [23]. The degree of change is also shown by the singular values S_n.

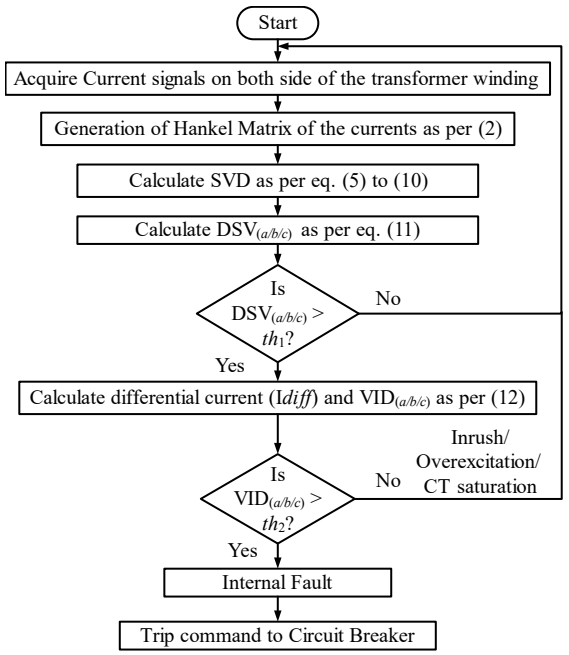

Fig. 1.The Proposed Protection Algorithm

III. THE PROPOSED PROTECTION SCHEME

The flowchart of the complete protection scheme is shown in Fig. 1. It is to be noted that the winding currents of both sides of the transformer winding are recorded. First, the SVD of the individual hankel matrix of the winding current is computed. During normal operation, the current will be sinusoidal and there will not be any discontinuity in the signal or its derivative. But, during the fault, due to change in current will be limited by the system inductance its derivative will have some value. Now, to get the first-order derivative (*k*-

1=1), we need to calculate second singular value of the signal. After calculating the singular values, the second singular value (DSV) difference is calculated for each phase as per (11).

$$\mathrm{DSV}_{(a/b/c)} = \left| S^{\mathrm{Prim}}_{2(a/b/c)} - S^{\mathrm{Sec}}_{2(a/b/c)} \right| \quad (11)$$

Where, $\mathrm{DSV}_{(a/b/c)}$ is the singular value difference of each phase. Similarly, $S^{\mathrm{Prim}}_{2(a/b/c)}$ and $S^{\mathrm{Sec}}_{2(a/b/c)}$ are the singular values of the individual phase currents of the primary and secondary sides of the transformer, respectively. The protection scheme detects a fault or abnormal condition when the DSV value exceeds a predefined threshold (th_1). After detection, the magnetizing inrush, overexcitation and the CT saturation during external through fault is sensed by calculating the variance of the normalised values of the differential current (VID) as per eq. (12) [24].

$$\mathrm{VID}_{(a/b/c)} = \sigma^2[\mathrm{norm}(\mathrm{I}diff_{(a/b/c)})] \quad (12)$$

Where, σ^2 represents the variance and 'norm' represents the normalisation of any dataset. Here, in this case, the variance of the normalised differential current (I*diff*) is considered and the same is calculated. During the magnetizing inrush, overexcitation and CT saturation during the external fault, the VID value remains well below the predefined threshold (th_2). For faulty conditions, the value of VID will be higher than the th_2 indicating the fault condition and a trip command to the circuit breaker is sent.

IV. Simulation and Threshold Selection

A. Simulation of the electrical network

In order to simulate the electrical network of the Gujarat Electricity Transmission and Corporation (GETCO), India, a simulation model has been created as depicted in Fig. 2. The appendix contains the data/parameters of the transformer. The sampling frequency of 4 kHz, which is the required sampling rate for the substation automation protocol IEC 61850, is used to acquire samples of CT secondary current of each side (primary and secondary side of the transformer) [25]. In the PSCAD/EMTDC software, the electrical network simulation model is created, and the MATLAB environment is used to create the protection system.

B. Simulated Cases

A large number of test cases are generated to evaluate the effectiveness of the developed protection scheme. The proposed scheme's performance is evaluated for all types of symmetrical (LLL and LLLG) and asymmetrical faults (LG, LL and LLG). Furthermore, the fault is created with varying fault inception angles, fault location (in terms of percentage of winding), and fault resistance variation. Magnetizing inrush cases are generated by varying the remanent flux and switching angle. Different external faults with CT saturation are also considered to validate the proposed scheme's performance. Furthermore, the change in generating system impedance is taken into account. Table I lists the various

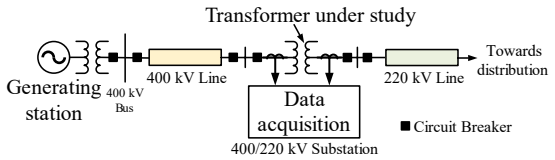

Fig. 2. Simulated Electrical Network of the GETCO, India

TABLE I. Parametric Variation Considered for Test Cases

Sr. No.	Parameter	Variation
1	Fault type	symmetrical (LLL and LLLG) and asymmetrical faults (LG, LL and LLG)
2	Fault Location	5%, 10%, 25%, 50%, 75% and 95% of the winding
3	Fault Inception angle and Switching angle	0˚, 30˚, 60˚, 90˚, and 120˚ of a reference phase (Phase-a)
4	Fault Resistance	5Ω, 10 Ω, 20Ω and 50Ω
5	Residual Flux	±5%, ±15%, ±25% and ±40%
6	Loading Condition	40%, 75% , 100% and 120%
7	System Impedance	8∠85°±2Ω

parametric variations considered for the generation of simulation cases in PSCAD/EMTDC.

C. Selection of thresholds

Because the currents have a sinusoidal waveform and there is no discontinuity in the signal or its derivative, there will be no change in current and the second singular value difference (DSV) will be zero during normal operation. During an internal fault, the value of the current signal changes, and even though the time series-current signal is continuous, the system inductance opposes the change, and the derivative of the signal has some value that will be reflected in terms of DSV. Because the currents at the transformer's ends will be similar during an external fault, the SVD value for both sides of the current will be the same, and the DSV will be zero. On the other hand, this DSV will be different in case of abnormal conditions like magnetizing inrush, overexcitation and the external fault with CT saturation. At that point, the variance of the normalised I*diff* is calculated. For a full and half sinusoidal waveform, these values will differ based on the waveform of the differential current (0.5 and 0.25). Eq. (13) calculates the variance, where N is the total sample count and '—' denotes the dataset's man value.

$$\sigma^2 = {}^{1}\!/_{\mathrm{N}} \sum_{i=1}^{\mathrm{N}} (\mathrm{I}diff(i) - \overline{\mathrm{I}diff})^2 \quad (13)$$

This value remains below 0.25 for the inrush current, overexcitation condition and external fault with CT saturation in all simulated cases [22]. This is because the waveform of the differential current will not be fully sinusoidal under these circumstances, resulting in a lower value of VID compared to the faulty situation with a fully sinusoidal waveform. As a result, the predefined threshold (th_2) for the VID is set at 0.25. Furthermore, the predefined threshold th_1 for the DSV should be chosen in such a way that the protection scheme can be selective. As a result, conditions such as magnetizing inrush current (2-5% of rated current), tap-changing (±5.5%) and maximum amplitude error of the CT (±5%) should be taken into account. Considering all of these conditions, a total error of 40% is considered for both sides of the transformer CT. Considering the appropriate safety margin, the th_1 can be selected as 0.5. Further, this margin can be adjusted based on the parameters of the protective system.

V. Results and Discussion

By adjusting the various factors, the proposed scheme's effectiveness is tested using generated simulation and various

situations (as per Table I). This section also discusses the in-depth study of the proposed scheme with differential protection.

A. Perforamcne during asymmetrical faults

Fig. 3 depicts the performance of the proposed method during LG and LL faults. With a fault inception angle of 0˚, the LG fault arises on a phase-A at 5% of the winding on the HV side. Fig. 3 (a) shows the performance of the suggested technique under these circumstances, which detects the fault in 5 ms. Fig. 3 (b) depicts the performance of differential protection for an identical situation, which takes around 20 ms (full-cycle). Similarly, the performance in the case of LL fault is shown in fig. 3 (c). Similarly, the performance in the case of LL fault is shown in fig. 3 (c). A LL fault occurs between A and C phases at 95% winding with a 30° fault initiation angle. The suggested technique detects LL faults in 4.75 ms, which is slower than the differential protection scheme shown in fig. 3. (d). The VID, in this case, remains well above th_2 due to entire sinusoidal waveform during fault.

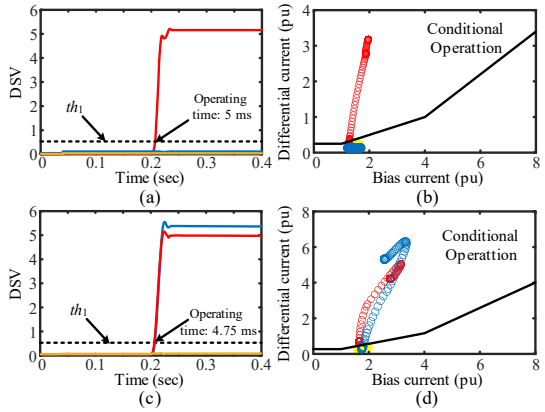

Fig. 3. Performance of the proposed method for (a) LG and (c) LL fault and performance of differential protection for (b) LG and (d) LL fault

B. Perforamcne during symmetrical faults

The proposed scheme's performance during symmetrical LLL fault is shown in Fig. 4. The LLL fault is simulated at 50% of the winding with a fault inception angle of the 60˚. The proposed scheme can detect the said fault within 4 ms as depicted in fig. 4 (a). For the same scenario, the performance of the differential protection scheme is shown in fig. 4 (b). The VID on this case remain well above th_2 due to full sinusoidal waveform during the fault.

C. Performance evaluation on real-field data

The proposed method's performance was evaluated using real-world data obtained via the CT secondary of the transformer protection scheme and made available as a relay

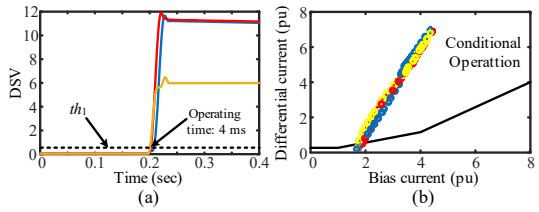

Fig. 4. Performance of the (a) proposed method and (b) differential protection for LLL fault

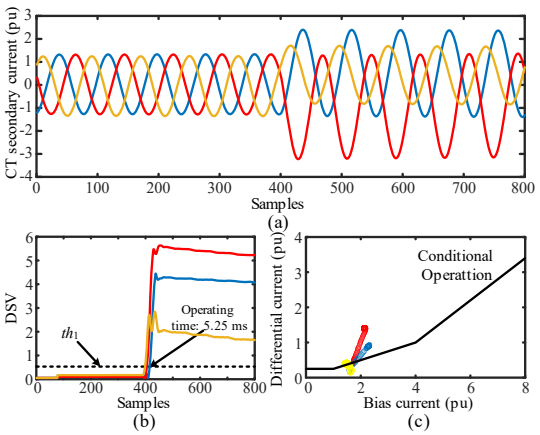

Fig. 5. Performance on real field data of LLL fault (a) CT secondary current, (b) DSV and (c) differential protection

COMTRADE file. For the LLL fault case, the operating times of the conventional differential protection scheme and the proposed technique are compared in fig. 5. The LLL fault data is obtained from an on-site 5 MVA, 33/11 kV, 50 Hz, Yd11 transformer. The analysis shows that the proposed method responds in 5.25 ms (from fig. 5 (b)) rather than the differential protection scheme's operating time of 20 ms (1 cycle) (from fig. 5 (c)). As a result, the proposed method outperforms the conventional method. The VID, in this case, remains well above th_2 due to the entire sinusoidal waveform during the LLL fault scenario.

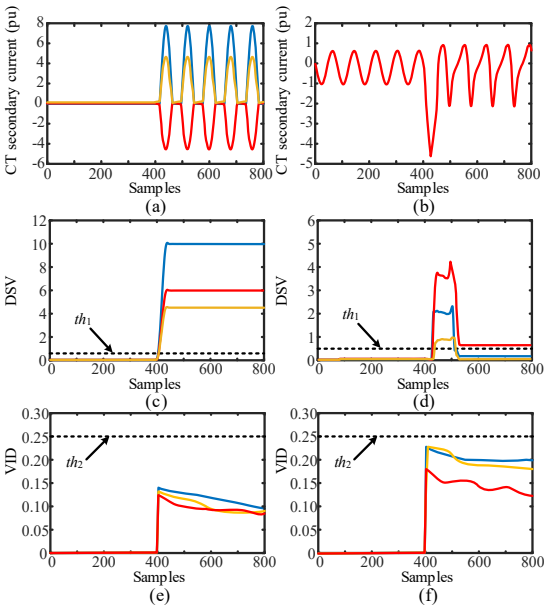

Fig. 6. Performance during inrush and CT saturation; (a), (b) CT secondary current, (c), (d) DSV and (e), (f) VID

D. Performance during inrush current and CT saturation during external fault

The suggested method's performance is tested for cases like inrush current and CT saturation during an external fault. As shown in fig. 6, the suggested strategy restrains its operation and maintains stability in both cases. Fig. 6 (a) and (b) represent the CT secondary current waveform in the case

of magnetic inrush and CT saturation conditions. Furthermore, the suggested scheme's performance in terms of DSV (fig. 6 (c) and (d)) and VID (fig 6. (e) and (f)) under magnetising inrush and CT saturation condition shows the stability of the proposed method during such scenarios.

VI. Conclusion

A novel approach based on singular value decomposition (SVD) is presented, which utilizes difference of SVDs from both sides (DSV) for the detection of fault conditions. The suggested approach detects symmetrical (LLL and LLLG) and asymmetrical (LG, LL, and LLG) faults in 5 ms, which is quicker than the standard differential protection's reaction time of 20 ms (1 cycle). Furthermore, separate criteria based on variance of normalised differential current (VID) is developed to ensure the stability of the protection scheme during abnormal operating conditions of the transformer like magnetising inrush, overexcitation, and CT saturation during external fault. The suggested scheme's performance is evaluated using a substantial amount of simulation cases (simulated on an existent electrical grid network) and real-field data. Moreover, the suggested technique can be easily retrofitted using the same equipment that is currently in use as it does not require additional components.

Appendix

Power transformer specification: Phase: 3, MVA: 315, Voltage level: 400 kV/220 kV, Frequency: 50 Hz, Connection: Yd1, Reactance (in terms of per phase): 12.5 %, Inrush current (percentage of rated current): 0.1%

Current transformer specification: Ratio: 1/433, Leakage Inductance: 0.8 mH, Burden resistance: 0.5 Ω

Acknowledgement

This work was supported by Central Power Research Institute as a research program under grant RSOP/2018/TR/03.

References

[1] Hitachi Energy, Application manual on Transformer protection RET670, version 2.2 IEC, 2022.

[2] "IEEE Guide for Protecting Power Transformers," in IEEE Std C37.91-2021 (Revision of IEEE Std C37.91-2008) , pp.1-160, 29 June 2021.

[3] Behrendt, Ken, Normann Fischer, and Casper Labuschagne. "Considerations for using harmonic blocking and harmonic restraint techniques on transformer differential relays." proceedings of the 33rd Annual Western Protective Relay Conference. 2006.

[4] S. Hodder, B. Kasztenny, N. Fischer and Y. Xia, "Low second-harmonic content in transformer inrush currents - Analysis and practical solutions for protection security," 2014 67th Annual Conference for Protective Relay Engineers, 2014, pp. 705-722.

[5] R. P. Medeiros, F. Bezerra Costa, K. Melo Silva, J. d. J. C. Muro, J. R. L. Júnior and M. Popov, "A Clarke-Wavelet-Based Time-Domain Power Transformer Differential Protection," IEEE Transactions on Power Delivery, vol. 37, no. 1, pp. 317-328, Feb. 2022.

[6] O. Ozgonenel and S. Karagol, "Transformer differential protection using wavelet transform," Electric Power Systems Research, vol. 114, pp. 60–67, 2014.

[7] S. R. Samantaray, B. K. Panigrahi, P. K. Dash, and G. Panda, "Power transformer protection using S-transform with complex window and pattern recognition approach," IET Generation Transmission Distribution, vol. 1, no. 2, pp. 278–286, 2007.

[8] M. Tajdinian and H. Samet, "Divergence Distance Based Index for Discriminating Inrush and Internal Fault Currents in Power Transformers," IEEE Transactions on Industrial Electronics, vol. 69, no. 5, pp. 5287-5294, May 2022

[9] Weng, Hanli, et al. "Discrete Fréchet distance algorithm based criterion of transformer differential protection with the immunity to saturation of current transformer." International Journal of Electrical Power & Energy Systems 115 (2020): 105449.

[10] Tajdinian, Mohsen, and Haidar Samet. "Application of probabilistic distance measures for inrush and internal fault currents discrimination in power transformer differential protection." Electric Power Systems Research 193 (2021): 107012.

[11] F. Haghjoo, M. Mostafaei and H. Mohammadi, "A New Leakage Flux-Based Technique for Turn-to-Turn Fault Protection and Faulty Region Identification in Transformers," IEEE Transactions on Power Delivery, vol. 33, no. 2, pp. 671-679, April 2018.

[12] O. Ozgonenel and S. Karagol, "Power transformer protection based on decision tree approach," IET Electric Power Applications, vol. 8, no. 7, pp. 251–256, 2014.

[13] A. M. Shah and B. R. Bhalja, "Discrimination Between Internal Faults and Other Disturbances in Transformer Using the Support Vector Machine-Based Protection Scheme," IEEE Transactions on Power Delivery, vol. 28, no. 3, pp. 1508-1515, July 2013.

[14] Kilic, Erdal, et al. "PCA based protection algorithm for transformer internal faults." Turkish Journal of Electrical Engineering and Computer Sciences, vol 17, no. 2, pp. 125-142, 2009.

[15] R. Naresh, V. Sharma and M. Vashisth, "An Integrated Neural Fuzzy Approach for Fault Diagnosis of Transformers," IEEE Transactions on Power Delivery, vol. 23, no. 4, pp. 2017-2024, Oct. 2008.

[16] A. M. Shah et al., "Quartile Based Differential Protection of Power Transformer," IEEE Transactions on Power Delivery, vol. 35, no. 5, pp. 2447-2458, Oct. 2020.

[17] T. Y. Ji, C. Mo, L. L. Zhang and Q. H. Wu, "Duty Cycle-Based Differential Protection Scheme for Power Transformers," IEEE Transactions on Power Delivery, vol. 37, no. 3, pp. 1380-1390, June 2022.

[18] H. S. Bhalja, B. R. Bhalja and P. Agarwal, "Rate of Rise of Differential Current Based Protection of Power Transformer," 2019 IEEE 16th India Council International Conference (INDICON), 2019, pp. 1-4.

[19] A. Ameli, M. Ghafouri, H. H. Zeineldin, M. M. A. Salama and E. F. El-Saadany, "Accurate Fault Diagnosis in Transformers Using an Auxiliary Current-Compensation-Based Framework for Differential Relays," IEEE Transactions on Instrumentation and Measurement, vol. 70, pp. 1-14, 2021.

[20] E. Ali, A. Helal, H. Desouki, K. Shebl, S. Abdelkader, and O. P. Malik, "Power transformer differential protection using current and voltage ratios," Elect. Power Syst. Res., vol. 154, pp. 140–150, Jan. 2018.

[21] O. Ozgonenel, E. Kilic, M. A. Khan, and M. A. Rahman, "A new method for fault detection and identification of incipient faults in power transformers," Electric Power Components and Systems, vol. 36, no. 11, pp. 1226–1244, 2008.

[22] O. Ozgonenel and E. Kilic, "Modeling and real-time fault identification in transformers," Journal of the Franklin Institute, vol. 345, no. 3, pp. 205–225, 2008.

[23] L. Zheng, K. Jia, B. Yang, T. Bi and Q. Yang, "Singular Value Decomposition Based Pilot Protection for Transmission Lines With Converters on Both Ends," IEEE Transactions on Power Delivery, vol. 37, no. 4, pp. 2728-2737, Aug. 2022.

[24] H. Esponda, E. Vázquez, M. A. Andrade and B. K. Johnson, "A Setting-Free Differential Protection for Power Transformers Based on Second Central Moment," IEEE Transactions on Power Delivery, vol. 34, no. 2, pp. 750-759, April 2019.

[25] "IEEE Recommended Practice for Implementing an IEC 61850-Based Substation Communications, Protection, Monitoring, and Control System," in IEEE Std 2030.100-2017 , pp.1-67, 19 June 2017.